Paramagnetic relaxivity of delocalized long-lived states of protons in chains of CH_2 groups

Aiky Razanahoera, Anna Sonnefeld, Geoffrey Bodenhausen, Kirill Sheberstov

Department of chemistry, École Normale Supérieure, PSL University, 75005 Paris, France

Correspondence to: Kirill Sheberstov, kirill.sheberstov@ens.psl.eu

Abstract. Long-lived states (LLS) have lifetimes T_{LLS} that can be much longer than longitudinal relaxation times ~~constants~~ T_1. In molecules containing several geminal pairs of protons in neighbouring CH_2 groups, it has been shown that *delocalized* ~~long-lived states~~ LLS can be excited by converting magnetization into imbalances between the populations of singlet and triplet states of each pair. Since the empirical yield of the conversion and reconversion of observable magnetization into LLS and back ~~are~~ is on the order of 10% ~~or less~~ if one uses spin-locked induced crossing (SLIC), it would be desirable to boost the sensitivity by dissolution dynamic nuclear polarization (d-DNP). To enhance the magnetization of nuclear spins by d-DNP, the analytes must be mixed with radicals such as 4-hydroxy-2,2,6,6-tetramethylpiperidin-1-oxyl (TEMPOL) ~~prior to freezing at low temperatures in the vicinity of 1 K~~. After dissolution, these radicals lead to an undesirable paramagnetic relaxation enhancement (PRE) which shortens not only the longitudinal relaxation times T_1 but also the lifetimes T_{LLS} of ~~long-lived states~~LLS. It is ~~confirmed~~ shown in this work that PRE by TEMPOL is less deleterious for LLS than for longitudinal magnetization, for four different molecules: 2,2-dimethyl-2-silapentane-5-sulfonate (DSS), homotaurine, taurine, and acetylcholine. The relaxivities r_{LLS} (i.e., the slopes of the relaxation ~~rates~~ rate constants R_{LLS} as a function of the radical concentration) ~~of LLS r_{LLS}~~ are 3 to 5 times smaller than the relaxivities r_1 of longitudinal magnetization ~~r_1~~. Partial delocalization of the LLS across neighbouring CH_2 groups may decrease this advantage, but in practice, this effect was observed to be ~~minor~~ small, for example when comparing taurine containing two CH_2 groups and homotaurine with three CH_2 groups. Regardless of whether the LLS are delocalized or not, it is shown that PRE should not be a major problem for experiments combining d-DNP and LLS, provided the concentration of paramagnetic species after dissolution does not exceed 1 mM, a condition that is readily fulfilled in typical d-DNP experiments. In bullet d-DNP experiments however, it may be necessary to decrease the concentration of ~~reduce~~ TEMPOL or ~~by~~ to add~~ing~~ ascorbate for chemical reduction ~~or using lower concentrations of TEMPOL~~.

Introduction

The lifetime of spin state populations~~s~~ in nuclear magnetic resonance (NMR) is normally limited by longitudinal relaxation. In certain cases, it is possible to access spin states that have extended lifetimes. ~~Usually, these are associated with~~In a coupled pairs of spins with $I = ½$, such ~~Such imbalances are also known as long-lived states (LLS). and correspond to population imbalances between singlet and triplet states of pairs of spins (Carravetta and Levitt, 2004; Carravetta et al., 2004).~~ long-lived

Formatted: Font color: Light Blue

Formatted: Font color: Light Blue

Formatted: Font color: Light Blue

Formatted: Font: Italic

Formatted: Font color: Red

Formatted: Font color: Light Blue

states (LLS) correspond to population imbalances between singlet and triplet states (Carravetta and Levitt, 2004; Carravetta et al., 2004) that. ~~Such imbalances are also known as long-lived states (LLS). They~~ are immune to intra-pair dipole-dipole interactions, which for pairs of protons are normally the dominant cause of longitudinal relaxation. In ~~multiple~~larger ~~spin~~ systems, ~~there can exist more LLS, such as those constituted by~~LLS may involve ~~four-spin and~~, ~~six~~ or more ~~-~~spins, all these states are weakly affected by dipolar relaxation ~~-scalar products-~~(Hogben et al., 2011). The relaxation time constants T_{LLS} can be much longer than typical longitudinal relaxation time constants T_1. This feature is particularly useful for protein-ligand studies (Salvi et al., 2012; Buratto et al., 2014b, 2016). Applications of LLS can be combined with different hyperpolarization methods, such as parahydrogen-based methods (Franzoni et al., 2012) or dissolution dynamic nuclear polarization (d-DNP) (Bornet et al., 2014; Kiryutin et al., 2019). D-DNP is the most universal method to achieve high spin polarization, and has found applications in drug screening (Lee et al., 2012; Buratto et al., 2014a; Kim et al., 2016), and in studies of metabolism by *in-vivo* magnetic resonance imaging (MRI) (Nelson et al., 2013). Before dissolution, the saturation of the electron spin transitions by micro-wave irradiation of a solid sample near 1 K leads to an enhancement of the nuclear spin polarization by up to 4 orders of magnitude, compared to the thermal polarization at room temperature in the same magnetic field. The sample is then quickly dissolved and transferred to a solution-state NMR spectrometer, where the high-resolution ~~signals~~ spectrum is ~~are~~ observed (Ardenkjær-Larsen et al., 2003). In an alternative approach known as "bullet DNP", the cold solid sample is ejected from the polarizer and rapidly transferred to the NMR spectrometer where it is dissolved (Kouřil et al., 2019). After dissolution, the unpaired electrons of the dilute paramagnetic agent give rise to undesirable paramagnetic relaxation enhancement (PRE). For most molecules of interest, such as metabolites or potential drugs, proton relaxation is fast so that the level of hyperpolarization suffers during dissolution and transfer, ~~which is the reason why d-DNP~~ which is one of the reasons why d-DNP is more often used for ^{13}C or ^{15}N rather than for protons. ~~Another benefit of using LLS for proton detection, is that it acts like a filter where the signal of interest is excited, and the proton background is suppressed.~~ Although molecules that are in enriched ^{13}C and ^{15}N offer many possibilities for the excitation of LLS (Feng et al., 2013; Elliott et al., 2019; Sheberstov et al., 2019), there are several drawbacks of using heteronuclei. Labelled compounds are expensive and ^{13}C or ^{15}N ~~NMR~~ observation is much less sensitive compared to ^{1}H. After converting proton LLS back into proton magnetization, only proton signals of interest are observed, while the background is suppressed. LLS involving pairs of protons often provide good contrast because protons are often directly exposed to the drug/target interface. On the other hand, the relaxation rate constants of ~~long-lived states~~LLS, ~~of protons~~ can be enhanced by mechanisms such as dipolar couplings to solvent nuclei, even with low gyromagnetic ratios, and to paramagnetic species (Kharkov et al., 2022).

Recently it was discovered that ~~proton~~ LLS involving geminal pairs of protons can be readily excited in many molecules containing at least two neighboring CH_2 groups (Sonnefeld et al., 2022a, b). Aliphatic chains, which are the focus of this study, are commonly found in potential drugs, so that LLS of CH_2 groups could provide a ~~breakthrough~~ new tool for drug screening using NMR. Hyphenation of LLS methodology with d-DNP offers promising perspectives, since at very low spin temperatures on the order of 10 mK that are routinely achieved in d-DNP, singlet-triplet imbalances can result from a violation of the high-temperature approximation, so that LLS ~~need not~~can be excited ~~by~~ without any radio-frequency (RF)

Formatted: Font color: Light Blue
Formatted: Font color: Light Blue
Formatted: Font color: Light Blue
Formatted: Font: Not Bold
Formatted: Font color: Light Blue
Formatted: Font color: Light Blue
Formatted: Font color: Light Blue
Formatted: Font color: Light Blue
Formatted: Font color: Light Blue
Formatted: Font color: Light Blue

irradiation (Tayler et al., 2012; Bornet et al., 2014; Kress et al., 2019). LLS that involve chemically equivalent proton pairs in CH_2 groups need not be sustained by RF fields or protected by shuttling to low fields. Therefore, one can transfer samples with hyperpolarized LLS ~~samples~~ to an NMR spectrometer for detection without significant losses of polarization. For small molecules, the ratios T_{LLS}/T_1 range typically from 2 to 6 for LLS~~s~~ in CH_2 groups in non-degassed samples (Sonnefeld et al., 2022a) although in some ~~cases in~~ degassed samples ~~and~~containing isolated ~~spin~~ pairs of ~~of either~~ protons (Sarkar et al., 2007) or carbon~~s~~-13 nuclei (Pileio et al., 2012; Stevanato et al., 2015) it is possible to achieve ~~the~~ ratios T_{LLS}/T_1 ~~ratios of above~~ > 30. In this work, we carried out a systematic analysis of relaxivities, i.e., of the dependence of the relaxation ~~rates~~ rate constants of LLS and longitudinal magnetization on the concentration of the paramagnetic species 4-hydroxy-2,2,6,6-tetramethylpiperidin-1-oxyl (TEMPOL).

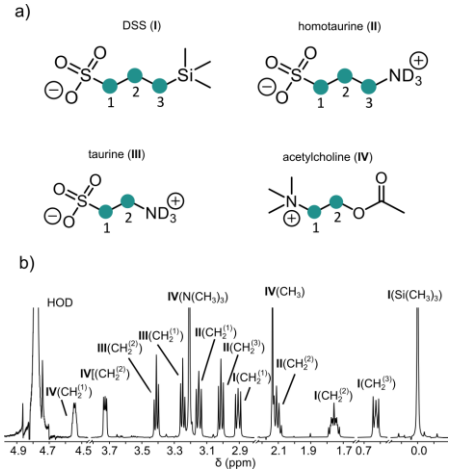

Figure 1. (a) Chemical structures of four molecules supporting LLS of CH_2 groups studied in this work: 2,2-Dimethyl-2-silapentane-5-sulfonate sodium salt (DSS, I), homotaurine (II), taurine (III), acetylcholine (IV). CH_2 groups supporting LLS are numbered in each structure and highlighted by green circles. (b) Assignment of the ^{1}H NMR spectrum of a mixture containing all four compounds.

Paramagnetic transition metal ions (Cu^{2+}, Mn^{2+}), lanthanides (Gd^{3+}) and triplet oxygen (O_2) have been shown to induce PRE of LLS, although PRE is not very efficient because the fluctuating external fields at the sites of two closely-spaced protons attached to the same carbon atom are strongly correlated (Tayler and Levitt, 2011). The effects of triplet oxygen on LLS have been ~~further~~ investigated in detail (Erriah and Elliott, 2019). The question arises if fluctuating external fields due to the bulky TEMPOL radical are ~~even~~ more strongly correlated than for paramagnetic ions or oxygen, in particular when they act on delocalized LLS involving several neighbouring CH_2 groups in the molecules ~~such as those~~ shown in Figure 1~~Figure 1~~. In DSS (I) and homotaurine (II), the LLS can be delocalized over all six protons of the three CH_2 groups, whereas in taurine (III) and acetylcholine (IV) the LLS always involves all four protons of both CH_2 groups. Titration experiments with TEMPOL

Formatted: Font color: Light Blue
Formatted: Font color: Light Blue
Formatted: Font color: Light Blue
Formatted: Font color: Light Blue
Formatted: Font color: Light Blue
Formatted: Font color: Red
Formatted: Font color: Light Blue

allowed us to determine to what extent the radical affects the LLS lifetimes and to determine whether it is necessary to quench the radicals after dissolution (Miéville et al., 2010). In low fields, in particular after dissolution during the transfer between the polarizer and the NMR magnet, PRE may be exacerbated by translational diffusion (Borah and Bryant, 1981) of the paramagnetic molecules relative to the analytes (Miéville et al., 2011).

Experimental methods

The delocalised LLS were excited by using spin-lock induced crossing (SLIC) (DeVience et al., 2013) and its polychromatic extension (Sonnefeld et al., 2022b). A generic SLIC pulse sequence is illustrated in Figure 2~~Figure 2~~a. After a non-selective 90º pulse that rotates the magnetization into the transverse plane, one, two or three continuous ~~selective spin-lock pulses~~ SLIC pulses with a common duration τ_{SLIC} are applied to the nuclei of interest, with a common RF amplitude (nutation frequency) ν_1 that matches a multiple of the geminal intra-pair J-coupling, i.e., $\nu_1 = n\, J^{intra}_{HH}$ with $n = 1$ for double- and $n = 2$ for single-quantum SLIC. ~~This leads to a population of the LLS through level~~ Level anti-crossings (LACs) ~~,~~ lead to a transfer of magnetization into LLS, i.e., into a ~~This~~ population imbalance between states with different permutation symmetry ~~is then allowed to relax during a delay τ_{rel}~~. Since pairs of protons in CH_2 groups are chemically equivalent in achiral molecules (i.e., have the same chemical shifts), and, in the absence of couplings to heteronuclei, are often nearly magnetically equivalent, there is no need to suppress singlet-to-triplet leakage by transporting the sample into a region of low magnetic field, or by applying an RF field to sustain the imbalance. ~~-~~After allowing the LLS to relax during a delay τ_{rel}, a T_{00} filter ~~designed to~~ removes shorted-lived terms (Tayler and Levitt, 2013; Tayler, 2020), and a second SLIC pulse reconverts the remaining LLS back into observable magnetization for detection. In this work, SLIC experiments with single, double, and triple irradiation (henceforth called "single, double, and triple SLIC experiments" for simplicity), ~~single, double, and triple SLIC experiments~~ were carried out to determine T_{LLS}, as shown by wavy arrows in Figure 2~~Figure 2~~b and c.

Formatted: Indent: First line: 1.25 cm

Formatted: Font color: Red

Formatted: Font: Italic

Formatted: Font: (Default) +Body (Times New Roman), Not Italic, Font color: Light Blue

Formatted: Font color: Light Blue

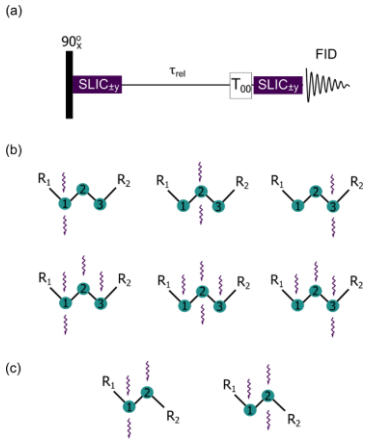

Figure 2. (a) Generic pulse sequence for single- and poly- spin-lock induced crossing (SLIC) where selective RF fields can be applied simultaneously to two or more CH_2 groups. (b) Six possible poly-SLIC experiments applied to molecules containing three CH_2 groups ~~(~~such as I and II of Fig. 1a~~)~~. The upper row shows three experiments with irradiation at a single ~~offset~~ frequency for the creation of LLS and a single readout pulse applied to the offset of the first, second or third CH_2 group; the lower row shows three experiments using triple irradiation of all three CH_2 groups for LLS excitation, combined with a single readout SLIC applied to only one of the three CH_2 groups. (c) Two schemes with double SLIC excitation and single SLIC readout for compounds containing only two CH_2 groups ~~(~~such as III and IV of Fig. 1a~~)~~.

Titrations were performed by preparing a set of samples where all compounds except TEMPOL had fixed concentrations. The volume of each sample was 600 µL. A stock solution with 40 mM of each compound was diluted by a factor 4 to obtain a final concentration of 10 mM for each compound~~. Each sample contained 10 mM of each compound in a 250 mM phosphate buffer phosphate buffer~~ in D_2O at pH 7.0 without removing paramagnetic oxygen by degassing. A stock solution of phosphate buffer (70 mM KH_2PO_4 and 130 mM K_2HPO_4) was prepared in D_2O and diluted by factor 4 ~~in each sample~~. A 20 mM TEMPOL stock solution was diluted in steps and added to yield final concentrations of 0.5, 1.0, 2.0, 3.0, 4.0, and 6.0 mM. The ^1H NMR spectra were obtained by adding ~~…~~16 signals (for experiments with single SLIC irradiation) ~~and~~or 8 signals (for experiments with multiple SLIC irradiation) ~~were recorded~~ using a 500 MHz AVANCE Neo Bruker spectrometer with a 5mm iProbe at 298 K. Each sample contained a mixture of all four molecules, thus ensuring accurate comparisons of relaxation ~~rates~~ rate constants of different molecules. The ~~assigned~~ ^1H NMR spectrum of the mixture with its assignments is presented in Figure 1~~Figure 1~~b. Typical signal decays due to LLS relaxation as a function of the TEMPOL concentration are shown in Figure 3~~Figure 3~~. The ~~Typical~~ intensities of the LLS-derived signals ~~is~~are typically ~~around~~about 5 % for single SLIC experiments and up to 10 % for poly-SLIC experiments. The theoretical maximum efficiency of LLS excitation and reconversion in a four-spin ~~system of~~ -CH_2-CH_2- moiety was ~~previously~~ calculated to be 14% for single SLIC ~~irradiation~~ and 28% for double SLIC experiments (Sonnefeld et al., 2022a). Simulations of the contributions of different LLS terms to the observed signals were performed ~~in~~ using SpinDynamica (Bengs and Levitt, 2018).

Formatted: Font color: Light Blue

Formatted: Font color: Light Blue

Formatted: Font color: Light Blue

Formatted: Font color: Light Blue, Subscript

Formatted: Font color: Light Blue

Formatted: Font color: Light Blue, Subscript

Formatted: Font color: Light Blue

Formatted: Font color: Light Blue

Formatted: Font color: Red

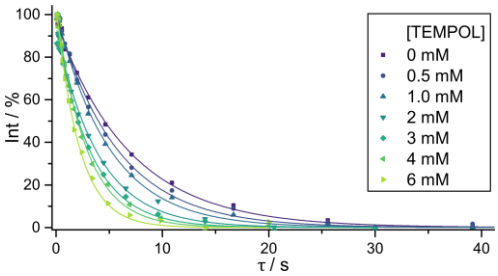

Figure 3. Decays of LLS-derived signals of DSS (compound I) for different TEMPOL concentrations. The LLS were excited and reconverted by irradiation with single SLIC pulses applied to $CH_2^{(1)}$ with an RF amplitude of 27 Hz to match the condition for single-quantum level anti-crossing (SQ LAC). The solid lines correspond to mono-exponential fits, scaled to begin at 100%.

Formatted: Font color: Light Blue

Results and discussion

1.1 Comparison of relaxivities of long-lived states and of longitudinal magnetization: partly correlated random fields

As apparent in Figure 4~~Figure 4~~, both the longitudinal relaxation rate constant $R_1 = 1/T_1$ and the long-lived relaxation rate constant $R_{LLS} = 1/T_{LLS}$ depend linearly on the concentration of TEMPOL (in units of M or mol/L):

Formatted: Font color: Light Blue

Formatted: Font color: Light Blue

$$R_1 = R_1^{(0)} + r_1\,[\mathrm{TEMPOL}],$$
$$R_{LLS} = R_{LLS}^{(0)} + r_{LLS}\,[\mathrm{TEMPOL}]. \qquad (1)$$

The slopes r_{LLS} and r_1 are known as *relaxivities* (in units of $M^{-1}s^{-1}$); the intercepts $R_1^{(0)}$ and $R_{LLS}^{(0)}$ are the ~~rates~~ rate constants determined in the absence of TEMPOL. Figure 4~~Figure 4~~ shows that variations of R_1 between neighboring CH_2 groups within each molecule are much smaller than variations ~~of those between different~~from one molecule to ~~another~~s. Whereas the T_1 values of small molecules correlate with the molecular ~~weight~~ mass – the larger molecule, the shorter T_1 – this is not true for T_{LLS}. In the absence of TEMPOL, the longest T_{LLS} of ca. 15 s was observed for compound III, whereas the shortest T_{LLS} of ca. 5 s was found for compound IV, although their T_1 relaxation times and ~~their~~ molecular masses are roughly the same, so that their correlation times should be similar. The difference of T_{LLS} may be explained by the presence of 12 methyl protons in compound IV, which cause faster relaxation of LLS.

Formatted: Font color: Light Blue

Wokaun and Ernst famously demonstrated that PRE is less efficient for relaxation of zero-quantum coherences than for single-and double-quantum coherences (Wokaun and Ernst, 1978). Tayler and Levitt demonstrated that a similar logic also applies to LLS: whereas longitudinal relaxation is enhanced by fluctuations of external local fields induced by unpaired electrons of radicals, an LLS involving two spins $\vec{I}_1$ and $\vec{I}_2$ is only relaxed by fluctuating external fields if these are *not* correlated. In general, the extent of correlation of the two fluctuating fields at the locations of the two spins $\vec{I}_1$ and $\vec{I}_2$ can be

Formatted: Indent: First line: 1.27 cm

characterized by the correlation coefficient $C = \langle \vec{B}_1 \cdot \vec{B}_2 \rangle / (B_1 B_2)$, where $B_i = \sqrt{\langle \vec{B}_i \cdot \vec{B}_i \rangle}$ is the mean (time-averaged) amplitude. Only the *uncorrelated* part of the two fluctuating fields given by $\langle \vec{B}_1 - \vec{B}_2 \rangle^2 = \left(B_1^2 + B_2^2 - 2\langle \vec{B}_1 \cdot \vec{B}_2 \rangle \right)$ contributes effectively to LLS relaxation (Tayler and Levitt, 2011). The smaller the radical, the closer it can approach one of the two geminal protons, hence the smaller the correlation coefficient C. It has been shown (Tayler and Levitt, 2011) that the ratio of relaxivities:

$$\kappa = r_{LLS}/r_1, \qquad (2)$$

is a characteristic measure of the correlation coefficient *C*; the smaller κ, the larger *C*. The experimental ratios κ for the (chemically inequivalent) protons of the CH_2 group in the (chiral) dipeptide alanine-glycine varied in the range $0.5 < \kappa < 0.3$ depending on the size of the paramagnetic agent (Tayler and Levitt, 2011). A similar ratio $\kappa = 0.36$ was observed for the CH_2 group in the terminal glycine residue of the tripeptide Ala–Gly–Gly for PRE caused by triplet oxygen (Erriah and Elliott, 2019).

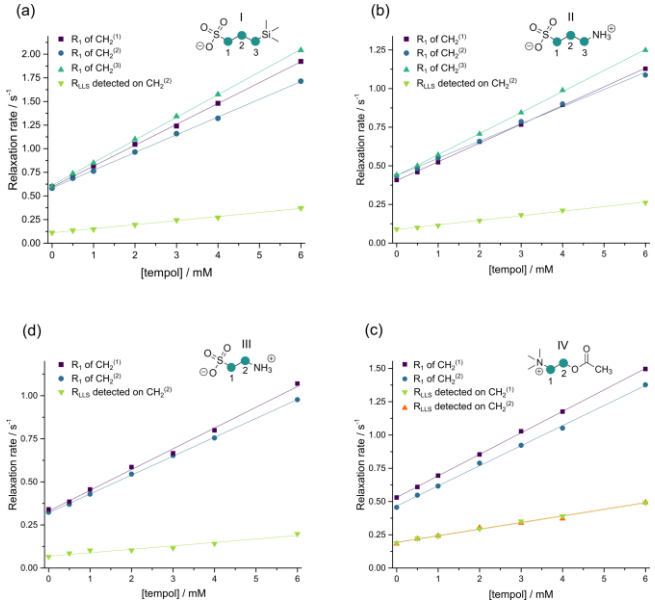

Figure 4. Relaxation rate constants $R_1 = 1/T_1$ and $R_{LLS} = 1/T_{LLS}$ in CH_2 groups of the four molecules I-IV as a function of the TEMPOL concentration. In (a) and (b), the LLS were excited by triple SLIC, in (c) and (d) by double SLIC, both with an RF amplitude of 13.5 Hz to match the condition for double-quantum level anti-crossing (DQ LAC.) In all cases, the LLS were reconverted into magnetization by single SLIC applied to the $CH_2^{(2)}$ group, except for compound IV, where two sets of experiments were with the reconversion performed with reconversion into magnetization of at theeither $CH_2^{(1)}$ and or at the $CH_2^{(2)}$ groups. The relaxivities r_1 and r_{LLS} correspond to the slopes of the linear regressions.

Formatted: Font color: Light Blue

In CH_2 chains with chemically equivalent pairs of protons in achiral molecules excited by exploiting magnetic inequivalence ~~in achiral molecules~~, the LLS can be delocalized over several CH_2 groups. Relaxation of an LLS localized within an individual CH_2 group will contribute to the decay of a delocalized LLS, so that one may expect the relaxivity of delocalized LLS to be more strongly affected by PRE than the relaxivity of a (hypothetical) localized LLS. We must however remain cautious, all the more since the longitudinal magnetizations of individual CH_2 groups may have a different relaxivities r_1. As we shall discuss below, the variations in the observed relaxivities r_{LLS} are not very large for different combinations of excitation and reconversion methods, and ~~these~~ intramolecular variations are much smaller than ~~the intermolecular~~ differences between distinct compounds, so that one can estimate an average ratio of relaxivities $\langle\kappa\rangle = \langle r_1\rangle/\langle r_{LLS}\rangle$ for all CH_2 groups in a given molecule. Compounds I-IV feature average ratios $\langle\kappa_{\mathrm{I}}\rangle \approx 0.22$, $\langle\kappa_{\mathrm{II}}\rangle \approx 0.23$, $\langle\kappa_{\mathrm{III}}\rangle \approx 0.18$, and $\langle\kappa_{\mathrm{IV}}\rangle \approx 0.32$ (see Table 1~~Table 1~~). Note the similarity of the ratios $\langle\kappa_{\mathrm{II}}\rangle$ and $\langle\kappa_{\mathrm{III}}\rangle$ obtained for compounds that differ by only one CH_2 group. The LLS can be delocalized to a variable extent between all three CH_2 groups in I and II, but are always equally distributed between the two CH_2 groups in compounds III and IV.

Table 1. Experimentally determined relaxation rates~~ constants~~ (s^{-1}) and relaxivities ($M^{-1}s^{-1}$). Standard errors determined from linear ~~fits~~ regressions are shown in parentheses. For double SLIC, the RF amplitude was chosen to match the condition for double-quantum level anti-crossing (LAC) ~~conditions~~, leading to different imbalances characterized by different ~~decay rates~~ rate constants $R_{LLS}^{(0)}$(SQ) with single SLIC excitation and single SLIC ~~reconversion~~ reconversion, and to rate constants $R_{LLS}^{(0)}$(DQ) with triple SLIC excitation and single SLIC reconversion.

Compound	$R_1^{(0)}$	$R_{LLS}^{(0)}$(SQ)	$R_{LLS}^{(0)}$(DQ)	r_1	r_{LLS}(SQ)	r_{LLS}(DQ)
I, $CH_2^{(1)}$	0.596(6)	0.144(2)	0.111(4)	0.221(2)	0.051(1)	0.043(1)
I, $CH_2^{(2)}$	0.585(6)	0.116(2)	0.106(3)	0.188(2)	0.046(1)	0.045(1)
I, $CH_2^{(3)}$	0.613(5)	0.125(3)	0.113(2)	0.240(2)	0.054(1)	0.048(1)
II, $CH_2^{(1)}$	0.405(4)	0.120(2)	0.093(3)	0.121(1)	0.029(1)	0.022(1)
II, $CH_2^{(2)}$	0.438(9)	0.102(3)	0.088(3)	0.111(3)	0.032(1)	0.030(1)
II, $CH_2^{(3)}$	0.437(3)	0.114(7)	0.089(3)	0.136(1)	0.032(2)	0.022(1)
III, $CH_2^{(1)}$	0.33(1)	-	-	0.120(3)	-	-
III, $CH_2^{(2)}$	0.321(3)	-	0.069(7)	0.109(1)	-	0.020(2)
IV, $CH_2^{(1)}$	0.532(4)	-	0.194(3)	0.162(1)	-	0.050(1)
IV, $CH_2^{(2)}$	0.467(8)	-	0.191(6)	0.151(3)	-	0.049(2)

Formatted: Font: 9 pt

Formatted: Font color: Light Blue

Formatted: Font color: Light Blue

1.2 Implications for dissolution DNP

Even though delocalized LLS are less affected by TEMPOL than longitudinal magnetization, the observed decrease in T_{LLS} is undesirable in the context of d-DNP. Since the use of TEMPOL or other polarizing agents is mandatory for d-DNP experiments, the question arises if it is worth scavenging TEMPOL after dissolution by addition of a reducing agent such as sodium ascorbate (vitamin C) to extend T_{LLS} after dissolution (Miéville et al., 2010, 2011). Note that the preparation of samples comprising two types of beads is rather cumbersome, ~~and has not been attempted so far~~in particular for bullet DNP. According to Miéville et al., the rate of the reduction of TEMPOL by sodium ascorbate may be slow on the time-scale of the transfer of the dissolved sample from the polarizer to the NMR magnet. Hence the reaction may not be entirely completed by the time the sample arrives in the spectrometer~~, and only a partial reduction of R_{LLS} may be achieved~~. Scavenging by sodium ascorbate may be accelerated ca. 100 times if one uses Frémy's salt instead of TEMPOL (Negroni et al., 2022). Several alternative approaches have been developed to remove radicals once DNP has been achieved. One approach is to use radicals obtained by UV irradiation of frozen pyruvic acid. These radicals are quenched as soon as the temperature increases (Eichhorn et al., 2013). One may also use radicals grafted ~~into~~ onto mesostructured silica materials (Gajan et al., 2014) or ~~onto~~ microporous polymers (Ji et al., 2017; El Daraï et al., 2021). However, the small relaxivities presented in Table 1~~Table 1~~ suggest that scavenging may not be necessary when using LLS ~~for the transport and~~to ~~preservation~~ preserve ~~of~~ the ~~spin~~ hyperpolarization.

1.3 Experiments and simulations for molecules with three CH_2 groups

It was shown (Sonnefeld et al., 2022b) that for the excitation of LLS in systems with n = 3 neighboring CH_2 groups, i.e., with $2n$ = 6 spins, there are 7 orthogonal LLS product operators that can be created, with 7 coefficients λ_i that depend on the excitation scheme:

$$\begin{aligned}\hat{\sigma}_{LLS} = {} & \left(-\lambda_{AA'}\hat{\mathbf{I}}^{A}\cdot\hat{\mathbf{I}}^{A'} - \lambda_{MM'}\hat{\mathbf{I}}^{M}\cdot\hat{\mathbf{I}}^{M'} - \lambda_{XX'}\hat{\mathbf{I}}^{X}\cdot\hat{\mathbf{I}}^{X'}\right) \\ & \left[-\lambda_{AA'MM'}\left(\hat{\mathbf{I}}^{A}\cdot\hat{\mathbf{I}}^{A'}\right)\left(\hat{\mathbf{I}}^{M}\cdot\hat{\mathbf{I}}^{M'}\right) - \lambda_{AA'XX'}\left(\hat{\mathbf{I}}^{A}\cdot\hat{\mathbf{I}}^{A'}\right)\left(\hat{\mathbf{I}}^{X}\cdot\hat{\mathbf{I}}^{X'}\right) - \lambda_{MM'XX'}\left(\hat{\mathbf{I}}^{M}\cdot\hat{\mathbf{I}}^{M'}\right)\left(\hat{\mathbf{I}}^{X}\cdot\hat{\mathbf{I}}^{X'}\right)\right] \\ & - \lambda_{AA'MM'XX'}\left(\hat{\mathbf{I}}^{A}\cdot\hat{\mathbf{I}}^{A'}\right)\left(\hat{\mathbf{I}}^{M}\cdot\hat{\mathbf{I}}^{M'}\right)\left(\hat{\mathbf{I}}^{X}\cdot\hat{\mathbf{I}}^{X'}\right),\end{aligned} \qquad (3)$$

Here A and A' denote the two protons of the $CH_2^{(1)}$ group, M and M' those of the middle $CH_2^{(2)}$ group, ~~and~~ while X and X' ~~those~~ correspond to ~~of~~ the terminal $CH_2^{(3)}$ group. This equation gives a general form of the density operator obtained after poly-SLIC, containing all long-lived terms found by numerical solution of the Liouville-von-Neumann equation. In addition to three bilinear terms, one encounters four higher terms that contain products of 4 and 6 spin operators. In principle, each term in Eq. (3~~(3~~) can decay with a different rate constant, so that one could distinguish up to 7 distinct rate constants~~s~~ $R_{LLS}^{(\mu)}$ with μ = AA', MM', XX', AA'MM', AA'XX', MM'XX' and AA'MM'XX'. ~~As was mentioned above,~~E ~~e~~ach term can ~~have~~ be excited with a different amplitude and can contribute with a different weight to the observed signal.

In systems such as compounds III and IV with only two CH_2 groups, only one LLS can be excited:

Formatted: Font color: Light Blue

Formatted: Font color: Light Blue

$$\hat{\sigma}_{LLS} = \left(-\lambda_{AA'}\hat{\mathbf{I}}^{A}\cdot\hat{\mathbf{I}}^{A'} - \lambda_{XX'}\hat{\mathbf{I}}^{X}\cdot\hat{\mathbf{I}}^{X'}\right) - \lambda_{AA'XX'}\left(\hat{\mathbf{I}}^{A}\cdot\hat{\mathbf{I}}^{A'}\right)\left(\hat{\mathbf{I}}^{X}\cdot\hat{\mathbf{I}}^{X'}\right), \quad (4)$$

The coefficients of the first two bilinear terms are always equal, i.e., $\lambda_{AA'} = \lambda_{XX'}$ while the 4-spin term is always proportional to ~~these~~ the leading bilinear terms, with a weight $\lambda_{AA'XX'} = 8/3\ \lambda_{AA'}$ (Sonnefeld et al., 2022a). This state corresponds to the imbalance between the singlet-singlet state and the triplet-triplet manifold and is therefore expected to decay monoexponentially. In two sets of complementary experiments performed for compound IV, the experimental relaxation rate constants~~s~~ were indeed found to be indistinguishable, as can be seen by comparing the red triangles and the green inverted triangles in Figure 4~~Figure 4~~d.

In compounds I and II however, which contain three adjacent CH_2 groups, different SLIC excitation schemes lead to ~~population~~ populate ~~of~~ different LLS, with different coefficients $\lambda_{LLS}^{(\mu)}$ in Eq. (3~~(3~~). There are 9 different ways of exciting miscellaneous LLS and 9 different ways of reconverting them, giving 81 possible experimental combinations. In order to investigate the relaxivities of these different LLS which may have different decay rate constants~~s~~ $R_{LLS}^{(\mu)}$ and different relaxivities $r_{LLS}^{(\mu)}$, we performed 6 different poly-SLIC experiments with different SLIC pulses for excitation and reconversion, and indeed found different LLS lifetimes (Figure 5~~Figure 5~~). Depending on the excitation and reconversion scheme used, there are pronounced differences between the relaxivities r_{LLS} within one and the same molecule.

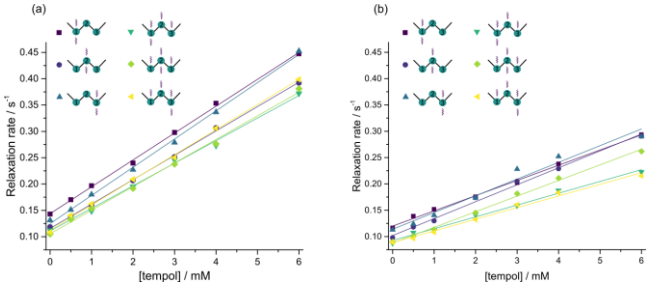

Figure 5. Decay rate constants~~s~~ $R_{LLS} = 1/T_{LLS}$ of long-lived states in CH_2 groups in (a) DSS (I) and (b) homotaurine (II), each containing three CH_2 groups, as a function of the TEMPOL concentration. Six different poly-SLIC experiments with distinct excitation and reconversion methods were performed for each molecule, as indicated by wavy arrows. The relaxivities r_{LLS} correspond to the slopes of the linear regressions.

We calculated the contributions of each of the 7 terms to the observable LLS-derived signals, after two consecutive transformations $\hat{I}_z^{in} \rightarrow \hat{\sigma}_{LLS} \rightarrow \hat{I}_x^{obs}$ (see Figure 6~~Figure 6~~). For each excitation scheme used in this work, we considered all 7 coefficients $\lambda_{\mu}^{M\rightarrow LLS}$ corresponding to the 7 terms in Eq. (3~~(3~~), as well as all 7 reconversion coefficients $\tilde{\lambda}_{\mu}^{LLS\rightarrow M}$. The coefficients are calculated according to:

$$\lambda_{\mu}^{M\rightarrow LLS}(\hat{I}_z^{in} \rightarrow \hat{\sigma}_{LLS}) = \frac{\mathrm{Tr}\{\hat{\rho}_{\mu}^{\dagger}\cdot\hat{\sigma}_{LLS}\}}{\mathrm{Tr}\{\hat{\rho}_{\mu}^{\dagger}\cdot\hat{\rho}_{\mu}\}}, \quad (5)$$

$$\tilde{\lambda}_{\mu}^{LLS\to M}(\hat{P}_{\mu} \to \hat{I}_{x,\mu}^{obs}) = \frac{\mathrm{Tr}\{\hat{I}_x^{\dagger}\hat{I}_{x,\mu}^{obs}\}}{\mathrm{Tr}\{\hat{I}_x^{\dagger}\cdot\hat{I}_x\}},$$

Here where the index μ corresponds to one of the 7 LLS terms in Eq. (3(3)), the operator $\hat{P}_{\mu}$ represents the LLS μ-th LLS term, $\hat{I}_z^{in}$ is the initial magnetization of the excited spins, $\hat{I}_x$ is the transverse magnetization of the observed spins after reconversion, and $\hat{I}_{x,\mu}^{obs}$ is the transverse magnetization obtained after reconversion of only the μ-th term $\hat{P}_{\mu}$ instead of the full $\hat{\sigma}_{LLS}$. The observed signal S_{μ} stemming from the μ^{th} term is determined by the product of two coefficients $\lambda_{\mu}^{M\to LLS}$ and $\tilde{\lambda}_{\mu}^{LLS\to M}$ for a given combination of excitation and reconversion SLIC pulses. These contributions are shown in Figure 6Figure 6. The sum of all all the7 7 amplitudes of all 7 combinations for each of excitation and reconversion SLIC schemepanel in Figure 6s was normalised to one. These graphs show how the LLSs are delocalized across the spin systems comprising n = 3 neighboring CH_2 groups. We only consider coherent spin dynamics during excitation and reconversion, neglecting possible redistributions of LLS due to Overhauser-type cross-relaxation effects, and neglecting zero- quantum coherences.

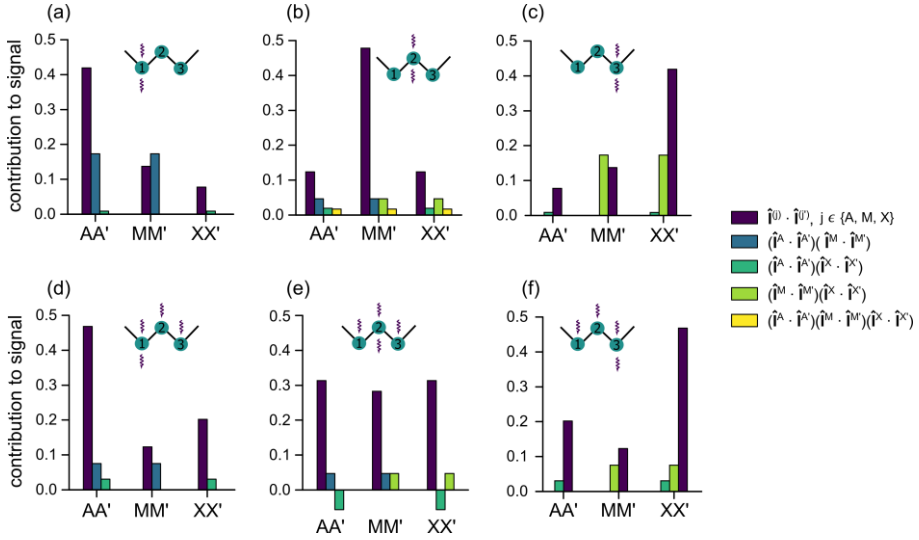

Figure 6. Calculated contributions of the seven 7 different LLS terms $\hat{P}_{\mu}$ (the three two-spin terms are shown in the same colour) in the density operator of Eq. (3(3)) to the observed signals for all 6 different single- and poly-SLIC experiments used in this work to determine the relaxivities $r_{LLS}^{(a)}$ in the 6-spin systems of DSS (I) and homotaurine (II). The histograms show the products $\lambda_{\mu}^{M\to LLS}\tilde{\lambda}_{\mu}^{LLS\to M}$ of the coefficients of LLS excitation and reconversion methods. The normalisation ensures that the sum of all products of coefficients is equal to 1. Experiments with triple SLIC excitation and single SLIC reconversion applied to the middle CH_2 group (e) provide LLS states that are almost evenly distributed among all three CH_2 groups, whereas the other experiments provide access to LLS states that are in part localised on the group where the reconversion SLIC pulse is applied. The excitation and reconversion of the (yellow) six-spin term is negligible except for case (b).

Formatted: Font: 9 pt

Note that a *single* SLIC pulse applied at the chemical shift of *any* of the three CH_2 groups results in the excitation of a delocalized state, which is predominantly (but not exclusively) associated with the irradiated pair. By using triple SLIC excitation and single SLIC reconversion applied to the middle CH_2 group, one can excite a fairly even distribution of ~~the~~ LLS involving all $2n = 6$ coupled spins. For compound II, the most strongly delocalized state features the largest relaxivity r_{LLS}. For compound I, however, the largest relaxivities were obtained for experiments where the largest contribution to the observed signal came from the terminal group $CH_2^{(3)}$~~, which~~ that is closest to the trimethylsilane group. This group has also the largest longitudinal relaxivity r_1, as can be seen in Figure 4~~Figure 4~~a. Detailed calculations of the relaxation superoperator might help to rationalize the experimental results obtained here.

Conclusions

The relaxation ~~rates~~ rate constants of various long-lived states and of the longitudinal magnetization of DSS, homotaurine, taurine and acetylcholine were measured as a function of the concentration of the radical TEMPOL. In all cases, the relaxivities r_{LLS} are lower by about a factor 3 compared to the relaxivities r_1. This implies that the effects of paramagnetic relaxation enhancement on LLS due to TEMPOL during sample transfer in dissolution ~~-~~DNP ~~sample transfer might be limited~~should not be too severe. Furthermore, the LLS relaxivity was studied ~~depending~~ for ~~on~~ different SLIC excitation and reconversion schemes. The results support simulations that show that different LLS are excited depending on ~~the number of adjacent methylene units in the molecule and~~ the SLIC sequence ~~used~~and the number of adjacent methylene units. SLIC methods have also been shown to be efficient for other achiral molecules containing neighboring CH_2 groups, such as dopamine, ~~taurine and~~ γ-aminobutyric acid (GABA), ethanolamine, and β-alanine (Sonnefeld, 2022a). All of these molecules contain aliphatic chains, so that the effects of paramagnetic polarizing agents like TEMPOL should be similar to what is reported in this work.

Formatted: Font color: Light Blue

Data availability

All original NMR data obtained for this paper is available through the Zenodo repository under https://doi.org/10.5281/zenodo.7432635

Conflict of interest

Geoffrey Bodenhausen is a member of the editorial board of the journal Magnetic Resonance of the Groupement Ampere. The peer-review process was guided by an independent editor. ~~T, and t~~The authors do not have ~~also no~~any other ~~competing~~ conflicting interests to declare.

Acknowledgements

We are indebted to the CNRS and the ENS for support, and to the European Research Council (ERC) for the Synergy grant "Highly Informative Drug Screening by Overcoming NMR Restrictions" (HISCORE, grant agreement number 951459).

Formatted: Font color: Light Blue

Formatted: English (United States)

References

Ardenkjær-Larsen, J. H., Fridlund, B., Gram, A., Hansson, G., Hansson, L., Lerche, M. H., Servin, R., Thaning, M., and Golman, K.: Increase in signal-to-noise ratio of > 10,000 times in liquid-state NMR, PNAS, 100, 10158–10163, https://doi.org/10.1073/pnas.1733835100, 2003.

Bengs, C. and Levitt, M. H.: SpinDynamica: Symbolic and numerical magnetic resonance in a Mathematica environment, Magn. Reson. Chem., 56, 374–414, https://doi.org/10.1002/mrc.4642, 2018.

Borah, B. and Bryant, R. G.: NMR relaxation dispersion in an aqueous nitroxide system, J. Chem. Phys., 75, 3297–3300, https://doi.org/10.1063/1.442480, 1981.

Bornet, A., Ji, X., Mammoli, D., Vuichoud, B., Milani, J., Bodenhausen, G., and Jannin, S.: Long-Lived States of Magnetically Equivalent Spins Populated by Dissolution-DNP and Revealed by Enzymatic Reactions, Eur. J. Chem., 20, 17113–17118, https://doi.org/10.1002/chem.201404967, 2014.

Buratto, R., Bornet, A., Milani, J., Mammoli, D., Vuichoud, B., Salvi, N., Singh, M., Laguerre, A., Passemard, S., Gerber-Lemaire, S., Jannin, S., and Bodenhausen, G.: Drug Screening Boosted by Hyperpolarized Long-Lived States in NMR, ChemMedChem, 9, 2509–2515, https://doi.org/10.1002/cmdc.201402214, 2014a.

Buratto, R., Mammoli, D., Chiarparin, E., Williams, G., and Bodenhausen, G.: Exploring Weak Ligand–Protein Interactions by Long-Lived NMR States: Improved Contrast in Fragment-Based Drug Screening, Angew. Chem. Int. Ed., 53, 11376–11380, https://doi.org/10.1002/anie.201404921, 2014b.

Buratto, R., Mammoli, D., Canet, E., and Bodenhausen, G.: Ligand–Protein Affinity Studies Using Long-Lived States of Fluorine-19 Nuclei, J. Med. Chem., 59, 1960–1966, https://doi.org/10.1021/acs.jmedchem.5b01583, 2016.

Carravetta, M. and Levitt, M. H.: Long-Lived Nuclear Spin States in High-Field Solution NMR, J. Am. Chem. Soc., 126, 6228–6229, https://doi.org/10.1021/ja0490931, 2004.

Carravetta, M., Johannessen, O. G., and Levitt, M. H.: Beyond the T1 Limit: Singlet Nuclear Spin States in Low Magnetic Fields, Phys. Rev. Lett., 92, 153003, https://doi.org/10.1103/PhysRevLett.92.153003, 2004.

DeVience, S. J., Walsworth, R. L., and Rosen, M. S.: Preparation of Nuclear Spin Singlet States Using Spin-Lock Induced Crossing, Phys. Rev. Lett., 111, 173002, https://doi.org/10.1103/PhysRevLett.111.173002, 2013.

Eichhorn, T. R., Takado, Y., Salameh, N., Capozzi, A., Cheng, T., Hyacinthe, J.-N., Mishkovsky, M., Roussel, C., and Comment, A.: Hyperpolarization without persistent radicals for in vivo real-time metabolic imaging, PNAS, 110, 18064–18069, https://doi.org/10.1073/pnas.1314928110, 2013.

El Daraï, T., Cousin, S. F., Stern, Q., Ceillier, M., Kempf, J., Eshchenko, D., Melzi, R., Schnell, M., Gremillard, L., Bornet, A., Milani, J., Vuichoud, B., Cala, O., Montarnal, D., and Jannin, S.: Porous functionalized polymers enable generating and transporting hyperpolarized mixtures of metabolites, Nat. Commun., 12, 4695, https://doi.org/10.1038/s41467-021-24279-2, 2021.

Elliott, S. J., Kadeřávek, P., Brown, L. J., Sabba, M., Glöggler, S., O'Leary, D. J., Brown, R. C. D., Ferrage, F., and Levitt, M. H.: Field-cycling long-lived-state NMR of 15N2 spin pairs, Mol. Phys., 117, 861–867, https://doi.org/10.1080/00268976.2018.1543906, 2019.

Erriah, B. and Elliott, S. J.: Experimental evidence for the role of paramagnetic oxygen concentration on the decay of long-lived nuclear spin order, RSC Adv., 9, 23418–23424, https://doi.org/10.1039/C9RA03748A, 2019.

Feng, Y., Theis, T., Liang, X., Wang, Q., Zhou, P., and Warren, W. S.: Storage of Hydrogen Spin Polarization in Long-Lived 13C2 Singlet Order and Implications for Hyperpolarized Magnetic Resonance Imaging, J. Am. Chem. Soc., 135, 9632–9635, https://doi.org/10.1021/ja404936p, 2013.

Franzoni, M. B., Buljubasich, L., Spiess, H. W., and Münnemann, K.: Long-Lived 1H Singlet Spin States Originating from Para-Hydrogen in Cs-Symmetric Molecules Stored for Minutes in High Magnetic Fields, J. Am. Chem. Soc., 134, 10393–10396, https://doi.org/10.1021/ja304285s, 2012.

Gajan, D., Bornet, A., Vuichoud, B., Milani, J., Melzi, R., van Kalkeren, H. A., Veyre, L., Thieuleux, C., Conley, M. P., Grüning, W. R., Schwarzwälder, M., Lesage, A., Copéret, C., Bodenhausen, G., Emsley, L., and Jannin, S.: Hybrid polarizing solids for pure hyperpolarized liquids through dissolution dynamic nuclear polarization, PNAS, 111, 14693–14697, https://doi.org/10.1073/pnas.1407730111, 2014.

Hogben, H. J., Hore, P. J., and Kuprov, I.: Multiple decoherence-free states in multi-spin systems, J. Magn. Reson., 211, 217–220, https://doi.org/10.1016/j.jmr.2011.06.001, 2011.

Ji, X., Bornet, A., Vuichoud, B., Milani, J., Gajan, D., Rossini, A. J., Emsley, L., Bodenhausen, G., and Jannin, S.: Transportable hyperpolarized metabolites, Nat. Commun., 8, 13975, https://doi.org/10.1038/ncomms13975, 2017.

Kharkov, B., Duan, X., Rantaharju, J., Sabba, M., Levitt, M. H., Canary, J. W., and Jerschow, A.: Weak nuclear spin singlet relaxation mechanisms revealed by experiment and computation, Phys. Chem. Chem. Phys., 24, 7531–7538, https://doi.org/10.1039/D1CP05537B, 2022.

Kim, Y., Liu, M., and Hilty, C.: Parallelized Ligand Screening Using Dissolution Dynamic Nuclear Polarization, Anal. Chem., 88, 11178–11183, https://doi.org/10.1021/acs.analchem.6b03382, 2016.

Kiryutin, A. S., Rodin, B. A., Yurkovskaya, A. V., Ivanov, K. L., Kurzbach, D., Jannin, S., Guarin, D., Abergel, D., and Bodenhausen, G.: Transport of hyperpolarized samples in dissolution-DNP experiments, Phys. Chem. Chem. Phys., 21, 13696–13705, https://doi.org/10.1039/C9CP02600B, 2019.

Kouřil, K., Kouřilová, H., Bartram, S., Levitt, M. H., and Meier, B.: Scalable dissolution-dynamic nuclear polarization with rapid transfer of a polarized solid, Nat. Commun., 10, 1733, https://doi.org/10.1038/s41467-019-09726-5, 2019.

Kress, T., Walrant, A., Bodenhausen, G., and Kurzbach, D.: Long-Lived States in Hyperpolarized Deuterated Methyl Groups Reveal Weak Binding of Small Molecules to Proteins, J. Phys. Chem. Lett., 10, 1523–1529, https://doi.org/10.1021/acs.jpclett.9b00149, 2019.

Lee, Y., Zeng, H., Ruedisser, S., Gossert, A. D., and Hilty, C.: Nuclear Magnetic Resonance of Hyperpolarized Fluorine for Characterization of Protein–Ligand Interactions, J. Am. Chem. Soc., 134, 17448–17451, https://doi.org/10.1021/ja308437h, 2012.

Miéville, P., Ahuja, P., Sarkar, R., Jannin, S., Vasos, P. R., Gerber-Lemaire, S., Mishkovsky, M., Comment, A., Gruetter, R., Ouari, O., Tordo, P., and Bodenhausen, G.: Scavenging Free Radicals To Preserve Enhancement and Extend Relaxation Times in NMR using Dynamic Nuclear Polarization, Angew. Chem. Int. Ed., 49, 6182–6185, https://doi.org/10.1002/anie.201000934, 2010.

Miéville, P., Jannin, S., and Bodenhausen, G.: Relaxometry of insensitive nuclei: Optimizing dissolution dynamic nuclear polarization, J. Magn. Reson., 210, 137–140, https://doi.org/10.1016/j.jmr.2011.02.006, 2011.

Negroni, M., Turhan, E., Kress, T., Ceillier, M., Jannin, S., and Kurzbach, D.: Frémy's Salt as a Low-Persistence Hyperpolarization Agent: Efficient Dynamic Nuclear Polarization Plus Rapid Radical Scavenging, J. Am. Chem. Soc., 144, 20680–20686, https://doi.org/10.1021/jacs.2c07960, 2022.

Nelson, S. J., Kurhanewicz, J., Vigneron, D. B., Larson, P. E. Z., Harzstark, A. L., Ferrone, M., van Criekinge, M., Chang, J. W., Bok, R., Park, I., Reed, G., Carvajal, L., Small, E. J., Munster, P., Weinberg, V. K., Ardenkjaer-Larsen, J. H., Chen, A. P., Hurd, R. E., Odegardstuen, L.-I., Robb, F. J., Tropp, J., and Murray, J. A.: Metabolic Imaging of Patients with Prostate Cancer Using Hyperpolarized [1-13C]Pyruvate, Sci. Transl. Med., 5, 198ra108, https://doi.org/10.1126/scitranslmed.3006070, 2013.

Pileio, G., Hill-Cousins, J. T., Mitchell, S., Kuprov, I., Brown, L. J., Brown, R. C. D., and Levitt, M. H.: Long-Lived Nuclear Singlet Order in Near-Equivalent 13C Spin Pairs, J. Am. Chem. Soc., 134, 17494–17497, https://doi.org/10.1021/ja3089873, 2012.

Salvi, N., Buratto, R., Bornet, A., Ulzega, S., Rentero Rebollo, I., Angelini, A., Heinis, C., and Bodenhausen, G.: Boosting the Sensitivity of Ligand–Protein Screening by NMR of Long-Lived States, J. Am. Chem. Soc., 134, 11076–11079, https://doi.org/10.1021/ja303301w, 2012.

Sarkar, R., Vasos, P. R., and Bodenhausen, G.: Singlet-State Exchange NMR Spectroscopy for the Study of Very Slow Dynamic Processes, J. Am. Chem. Soc., 129, 328–334, https://doi.org/10.1021/ja0647396, 2007.

Sheberstov, K. F., Vieth, H.-M., Zimmermann, H., Rodin, B. A., Ivanov, K. L., Kiryutin, A. S., and Yurkovskaya, A. V.: Generating and sustaining long-lived spin states in 15 N, 15 N′-azobenzene, Sci. Rep., 9, 20161, https://doi.org/10.1038/s41598-019-56734-y, 2019.

Sonnefeld, A., Razanahoera, A., Pelupessy, P., Bodenhausen, G., and Sheberstov, K.: Long-lived states of methylene protons in achiral molecules, Sci. Adv., 8, eade2113, https://doi.org/10.1126/sciadv.ade2113, 2022a.

Sonnefeld, A., Bodenhausen, G., and Sheberstov, K.: Polychromatic Excitation of Delocalized Long-Lived Proton Spin States in Aliphatic Chains, Phys. Rev. Lett., 129, 183203, https://doi.org/10.1103/PhysRevLett.129.183203, 2022b.

Stevanato, G., Hill-Cousins, J. T., Håkansson, P., Roy, S. S., Brown, L. J., Brown, R. C. D., Pileio, G., and Levitt, M. H.: A Nuclear Singlet Lifetime of More than One Hour in Room-Temperature Solution, Angew. Chem. Int. Ed., 54, 3740–3743, https://doi.org/10.1002/anie.201411978, 2015.

Tayler, M. C. D.: Chapter 10: Filters for Long-lived Spin Order, in: Long-lived Nuclear Spin Order, The Royal Society of Chemistry, 188–208, https://doi.org/10.1039/9781788019972-00188, 2020.

Tayler, M. C. D. and Levitt, M. H.: Paramagnetic relaxation of nuclear singlet states, Phys. Chem. Chem. Phys., 13, 9128–9130, https://doi.org/10.1039/C1CP20471H, 2011.

Tayler, M. C. D. and Levitt, M. H.: Accessing Long-Lived Nuclear Spin Order by Isotope-Induced Symmetry Breaking, J. Am. Chem. Soc., 135, 2120–2123, https://doi.org/10.1021/ja312227h, 2013.

Tayler, M. C. D., Marco-Rius, I., Kettunen, M. I., Brindle, K. M., Levitt, M. H., and Pileio, G.: Direct Enhancement of Nuclear Singlet Order by Dynamic Nuclear Polarization, J. Am. Chem. Soc., 134, 7668–7671, https://doi.org/10.1021/ja302814e, 2012.

Wokaun, A. and Ernst, R. R.: The use of multiple quantum transitions for relaxation studies in coupled spin systems, Mol. Phys., 36, 317–341, https://doi.org/10.1080/00268977800101601, 1978.